

See discussions, stats, and author profiles for this publication at: <https://www.researchgate.net/publication/259993681>

Low temperature thermal conductivity of aluminum alloy 5056

Article in *Cryogenics* · March 2014

DOI: 10.1016/j.cryogenics.2013.12.008

CITATIONS

8

READS

1,344

2 authors:



Bertrand Baudouy

Atomic Energy and Alternative Energies Commission

113 PUBLICATIONS 735 CITATIONS

[SEE PROFILE](#)



Aurélien Four

Atomic Energy and Alternative Energies Commission

18 PUBLICATIONS 72 CITATIONS

[SEE PROFILE](#)

Some of the authors of this publication are also working on these related projects:



Transient heat transfer in boiling helium natural circulation loops [View project](#)



FRESCA2 [View project](#)

Low temperature thermal conductivity of aluminum alloy 5056

B. Baudouy, A. Four

CEA Saclay, Irfu/SACM, F-91191 Gif-sur-Yvette Cedex, France

Abstract

The thermal conductivity of 5056 aluminum alloy was determined from 4.2 K to 120 K using a differential steady-state method. This method has been implemented in a low temperature cryostat using a GM cryocooler as heat sink. The thermal conductivity of the 5056 aluminum alloy was determined since it was considered to be a part of a thermal link for the Planck research satellite. As expected, below 10 K the thermal conductivity is exclusively given by the electron defect scattering term. At higher temperature, the other terms from the electronic and the lattice contributions come into play but the electronic thermal conductivity term is still dominant. A workable fit, based on theory, is presented and can be used up to 300 K. Our measurements are compared with data at lower temperature and available fits from the literature.

Keywords: Thermal conductivity, aluminum alloy, Al 5056, low temperature

1. Introduction

In the aerospace or physics applications, low mass density materials with high thermal conductivities such as aluminum alloys are used to create thermal links at low temperature. There are several aluminum alloys that undergo different thermal and mechanical treatments depending on the applications. The Al 5056 alloy belongs to the 5000 series which are alloyed

with magnesium. It contains 5.2% of magnesium, 0.1% of Mn, 0.1% of Cr in weight and some other impurities. It is often used as thermal links in physics experiments at very low temperature [1, 2] and is also considered as a good conductor and structural material in the construction of the Planck telescope among other aluminum alloys [3]. Coccia *et al.* reported thermal conductivity data of Al 5056 between 0.05 and 1.3 K [4]. To the best of our knowledge, these are the sole thermal conductivity data reported in the literature for this alloy. Here, we present thermal conductivity of the alloy Al 5056 H39 at a higher temperature range from 4.2 K to 130 K using a steady state differential method. H39 denominates strain hardening and stabilizing by low temperature heating giving a high degree of hardness.

2. Determination procedure and experimental set-up description

2.1. Differential method

We measured the thermal conductivity with a 1D steady-state differential method, for which the relationship between the heat flux and the temperature gradient is given by the Fourier law $\vec{q} = -k(T)\vec{\nabla}T$ where q is the heat flux density and $k(T)$ the thermal conductivity; a function of temperature. When the cross-sectional area of the domain is constant, the integration of the Fourier law gives by definition the average value of the thermal conductivity $\overline{k(T)}$

$$\overline{k(T)} = \frac{1}{T_h - T_c} \int_{T_c}^{T_h} k(T) dT = \frac{Q}{T_h - T_c} \frac{l}{S}, \quad (1)$$

where Q is the heat flux dissipated across the sample, S the cross-sectional area, l the distance between the cold (T_c) and hot (T_h) temperature measurement locations. Equation (1) defines the average value of the thermal conductivity within the temperature range of measurement but for simplicity we assume that it is equivalent to the thermal conductivity at the average

temperature of the measurement range, *i.e.* $\bar{T} = (T_h + T_c) / 2$. This assumption introduces a systematic error, $\overline{k(T)} - k(\bar{T})$, which is small for $T_c \approx T_h$ and even vanishes when $T_c \rightarrow T_h$. In our measurements we imposed $\Delta T = T_h - T_c$ around 0.05 to 0.3 K, sufficiently small to neglect the systematic error introduced by the average value simplification.

2.2 Experimental set-up and procedure

The experimental set up is based on a vertically oriented vacuum can cryostat with a Gifford-McMahon cryocooler serving as cold source and located on the top flange. The second stage of the cryocooler has the capability of maintaining 4.2 K under a heat load of 1.5 W. The samples are thin tapes clamped between two high-purity copper blocks with copper-charged grease as described in [5]. Each copper block is instrumented with a calibrated Cernox 1050 temperature sensor, mounted also with copper-charged grease in small cavities. The upper copper block is associated with the measurement of T_c and the lower one with T_h as described in Figure 1. The lower copper block is heated to T_h with a Manganin® wire heater (Q -heater) wound around it while the lower copper block is maintained at T_c . The measurement part of the rig, *i.e.* the two copper blocks and the sample, is surrounded by a high purity copper radiation shield. The copper shield is 3 mm thick to ensure a constant temperature over the entire volume. The copper shield is separated from the second stage of the cryocooler by a thermal insert and a heater (see Fig. 1). The purpose of the insert is control the T_c temperature over a large temperature range with a reasonable power input to protect the second stage of the cryocooler from excessive power. This thermal insert was designed to have a 300 K temperature different across it while dissipating 12 W. The copper shield is further surrounded by an aluminum radiation, thermally anchored at the first stage. Both radiation shields have a superinsulation blanket located on their exterior.

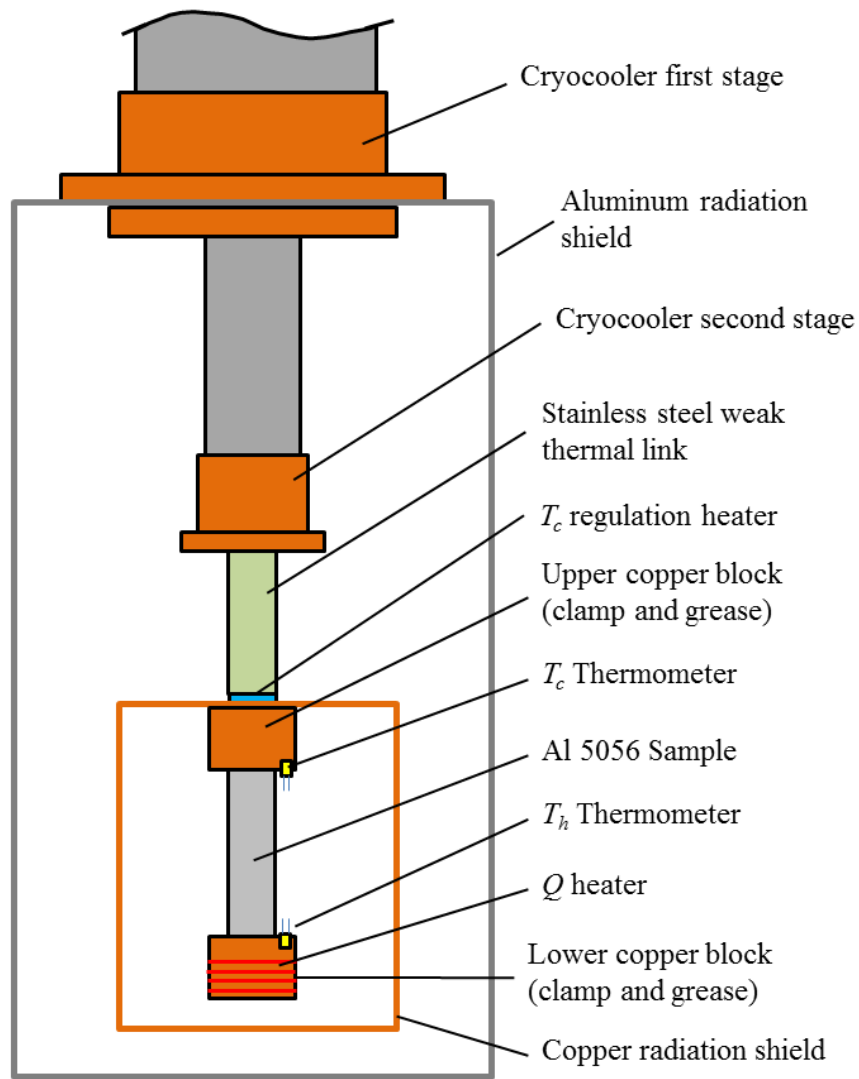


Figure 1. Schematic of the measurement part of the thermal conductivity rig

While T_c is maintained constant by the mean of the thermal insert heater, the power through the Q -heater is controlled to generate the temperature difference across the sample, ΔT . Repeated measurements were made at different T_c values with ΔT varying between 0.05 and 0.3 K. The data are recorded when the value of both temperatures become stable within a mK. The temperature stabilization can take several minutes at low temperature and up to an hour or longer at higher temperatures.

The electron mean free path in Al alloy $0.06\text{ }\mu\text{m}$ at 4 K, is much smaller than the smallest dimension of the samples. Thus there is no 2D effect on the electron scattering.

2.3 Experimental errors

The dimensions of the sample are measured at room temperature and their values at low temperature are estimated from the thermal contraction data [6]. Table 1 gathers the sample dimensions and their precision. The uncertainties in thermal contraction data are around 10% and the thermal contraction of aluminum alloy are at most 0.5% in the temperature range of the experiment. Thus the uncertainty induced by the thermal contraction is negligible compared to that incurred in the determination of the dimension of the sample (7% for the thickness).

The two Cernox® sensors were calibrated by Lakeshore Cryotronics. The error in the temperature measurement ranges from 2 mK at 4 K to 10 mK at 120 K due to the difference between the calibration fit and the data and the electronic chain. We also estimated the systematic error in the temperature measurements due to the thermal resistance between the copper blocks and the grease. Previous calculations estimated this temperature difference to be around 1 mK for a ΔT in the order of 50 K across the sample [3]. However, with the differential method, the ΔT across the samples is always lower than 0.3 K, therefore this systematic error is neglected in the rest of the error analysis.

The total heat flux, Q , is generated and monitored by a Keithley 2400 sourcemeter and the uncertainty is at most 0.5% of the value.

The typical relative measurement error value of the parameters constituting Eq. (1) are gathered in table 2. The main contribution to the thermal conductivity uncertainty is due to the temperature measurement uncertainty and that of the sample thickness.

Conduction through the instrumentation wiring and radiation heat losses must be examined as well as they can constitute systematic errors. From room temperature to the copper radiation shield, all the wires are PTFE insulated twisted pair OFHC cooper wire with an AWG of 30. The wires are thermally anchored onto the two radiation shields (aluminum and copper). From the copper radiation shield, several other wires are used. For the heater, a Constantan® twisted pair of 0.2 mm in diameter wire is used for the voltage measurement and a twisted pair Manganin® wire of 0.65 mm diameter for the current. Both wires are 1 meter long. For both thermometers, the wiring is composed of 2-m long twisted pair of 0.152 mm diameter Ph-Br wires. All wires, within the copper radiation shield, are installed in a pig tail manner to avoid any contact with the cooper shield. The wiring of the T_c sensor is thermally anchored to the copper shield and as the copper shield temperature is regulated at T_c or very close, the heat losses through the T_c sensor wiring is considered negligible. The maximum value of the conductive heat load on the sample is around 0.8 μW for a temperature of 22 K. The conductive heat load is two to four orders of magnitude lower than Q and therefore will be neglected in the error analysis.

The radiation heat losses from the copper shield surrounding the samples are also neglected since by construction the copper shield and the sample temperatures are quasi-identical within ΔT .

Finally, the error (σ_k) in the determination of k is given by the error propagation equation [7] as $(\sigma_k/k)^2 = (\sigma_Q/Q)^2 + (\sigma_l/l)^2 + (\sigma_S/S)^2 + (\sigma_{\Delta T}/\Delta T)^2$ and it is reported in the Table 3 with the thermal conductivity data. On average, the error in the determination of the thermal conductivity is

around 10% with a maximum of 17% at 55 K due to small ΔT imposed to the sample ($\Delta T=0.1$ K).

3. Experimental results and analysis

Figure 2 depicts the evolution of the thermal conductivity of the Al 5056 sample as a function of temperature (data from the table 3). The evolution of the thermal conductivity with the temperature is typical of diluted alloy metal [6]. At the lowest temperature, the thermal conductivity is dominated by the electronic thermal conduction. Its evolution with temperature is linear since the electron defect scattering thermal resistance (R_0) is controlling the heat transport mechanism. At higher temperature, the electronic thermal transport is limited by electron-phonon scattering. The associated thermal resistance varies as $R_L \propto T^n$ and is an intrinsic characteristic of each metal as it is independent on imperfections and impurities. The theory gives $n=2$ but experimentally is found to vary up to 3. For different dilute alloys, Powell found that the exponent of the electron- phonon scattering resistance is closer to 3 ($n=2.72$) [8]. The electronic thermal conductivity is defined as the inverse of the sum of the thermal resistances defined above and a deviation term that is a combination of these two resistances [8, 9] as

$$\frac{1}{k_e} \approx R_L + R_0 + R_{L0} = A.T^n + B/T + \alpha \cdot \frac{R_L.R_0}{\beta.R_L + \gamma.R_0}. \quad (2)$$

A , B , α , β and γ are adjustable parameters. The alloy Al 5056 includes several percent of other components than aluminum and the thermal conductivity cannot be modeled only by the electronic contribution. As the electronic thermal conduction decreases with temperature, the lattice component of the thermal conductivity, k_l , is not negligible even if it is lower than the electronic contribution. For lightly alloyed metal, such as Al 5056, the lattice contribution to

the thermal conductivity is limited by three main phenomena. The scattering of the lattice waves by the electrons and by dislocations are two of them and their associated thermal resistances have the same temperature dependency in T^{-2} . The third one is the scattering by lattice imperfections for which the resistance goes as T [6, 10]. The lattice thermal conductivity is described by,

$$\frac{1}{k_l} \approx E.T^{-2} + F.T, \quad (3)$$

where E and F are also adjustable parameters. The total thermal conductivity is the sum of both contributions

$$k = k_e + k_l, \quad (4)$$

Equation (4) (with eq. (2) and (3)) is also plotted in figure 2 between 1 K and 300 K as a solid line. The different parameters used in equations (2) and (3) to adjust equation (4) to the data are listed in table 4. The numerical results of equation (4) are listed in table 3. For the electronic term (Eq. (2)), the coefficient B has been obtained by fitting the experimental data below 20 K since this term is dominant at low temperature. For the electron phonon scattering term we decided to use the parameters found by Powell that is to say $n=2.72$ and $A=2.03 \cdot 10^{-8} \text{ m K}^{n+1}/\text{W}$ since this term is an intrinsic characteristic of each metal. Moreover these value were used by Powell for different commercial aluminum alloy [8]. For the deviation term in Eq. (2), the coefficients α , β and γ were left free but bounded between 0 and 2 as described by the theory. The lattice component coefficients E and F were also left free. The value of the adjustable parameters (α , β , γ , E and F .) are similar to what Powell found for the alloy 5083-O and 5086-F. The average deviation between (4) and the data is 4% with a maximum deviation of 12% for 95 K for where our thermal conductivity value seems rather small. Equation (4) has been extended from 1 K and up to 300 K for comparison with the measurement of Coccia

et al [4] and the Woodcraft's fitting method [11]. We depict the result of Coccia's at 1 K (black circle in figure 2) and the difference with our fit is 2%. The fit from Woodcraft's method (dashed line) has been produced in using a thermal conductivity value of 3.5 W/mK at 4 K. The average difference between Woodcraft's curve and our fit is 4% over the temperature range of investigation with a maximum deviation of 5%. From 1 K to 300 K, the average difference is reduced to 3%.

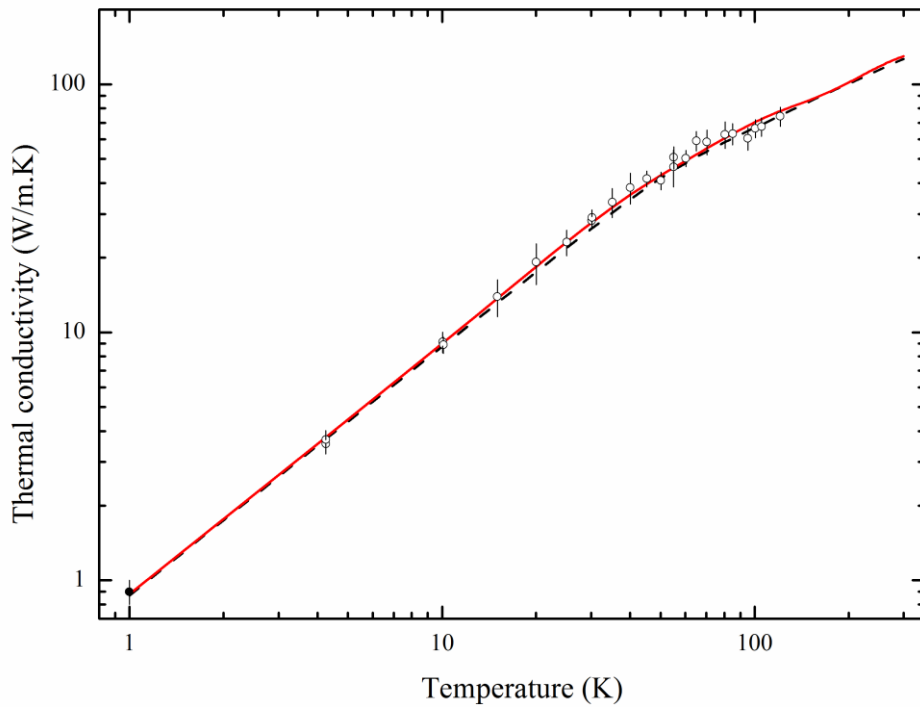


Figure 2. Thermal conductivity evolution as a function of temperature for Al 5056. The symbols \circ represent our experimental data and \bullet represent Coccia's measurement [4]. The solid line is equation (4). The dashed line is the numerical data given by the fitting method of Woodcraft [11].

4. Conclusions

The thermal conductivity of the aluminum alloys 5056 H39, was measured with a differential method with an experimental error in the order of 10% from 4 K to 120 K. Based on the theory of thermal conductivity, we propose a fit of the temperature evolution of the thermal conductivity of the Al 5056. The adjustable parameters are in good agreement with other aluminum alloy data. Our fit is also in good agreement with the Woodcraft's prediction and can be used between 1 K to 300 K with a good accuracy.

Acknowledgements

This work was funded by RUAG Space, RUAG Schweiz AG, Schaffhauserstrasse 580, 8052 Zürich, Switzerland.

References

- [1] Barucci M, et al. Very low temperature specific heat of Al 5056. *Physica B: Condensed Matter*. 2010;405(6):1452-4.
- [2] Coccia E, Modena I. Smooth heat switch below 1 K. *Cryogenics*. 1993;33(2):228-9.
- [3] Baudouy B. Low temperature thermal conductivity of aluminum alloy 1200. *Cryogenics*. 2011;51(11-12):617-20
- [4] Coccia E, Niinikoski TO. Thermal and superconducting properties of an aluminium alloy for gravitational wave antennae below 1K *J Phys E: Sci Instrum*. 1983;16(7):595-9.
- [5] McDonald PC, et al. Thermal validation of the design of the CFRP support struts to be used in the spatial framework of the Herschel Space Observatory. *Cryogenics*. 2006;46:298-304.
- [6] Reed RP, Clark AF. *Materials at low temperatures*. Metal Park, Ohio, USA: American Society for materials; 1983.
- [7] Bevington PR, Robinson DK. *Data reduction and error analysis for the physical sciences*. 2nd ed: WCB McGraw-Hill; 1992.
- [8] Powell RL, et al. Low-Temperature Transport Properties of Commercial Metals and Alloys. II. Aluminums. *Journal of Applied Physics*. 1960;31(3):496-503.
- [9] Powell RL, et al. Low-temperature transport properties of copper and its dilute alloys : Pure copper, annealed and cold-drawn. *Physical review*. 1959;115(2):314-23.
- [10] Ho CY, et al. Thermal Conductivity of elements : A comprehensive review. *Journal of Physical and Chemical Data*. 1974;3(Suppl. n° 1):1-796.
- [11] Woodcraft AL. Predicting the thermal conductivity of aluminium alloys in the cryogenic to room temperature range. *Cryogenics*. 2005;45(6):421-31.